

Strength Analysis of Lap Joints in Aerospace Structural Materials

Mariusz Kłonica^{1*}, Rafał Chatys², Ilmars Blumbergs³

¹ Faculty of Mechanical Engineering, Department of Production Engineering, Lublin University of Technology, ul. Nadbystrzycka 36, 20-618 Lublin, Poland

² Faculty of Mechatronics and Machine Design, Kielce University of Technology, Al. 1000-lecia P.P.725-314 Kielce, Poland

³ Institute of Aeronautics, Faculty of Mechanical Engineering, Transport and Aeronautics, Riga Technical University, ul. Ķīpsalas 6B, Kurzemes rajons, LV-1048, Riga, Latvia

* Corresponding author's e-mail: m.klonica@pollub.pl

ABSTRACT

This paper is a study on the results of strength tests on single-lap joints used primarily in the aerospace industry, based on a Hi-Lok fastener. Two popular structural materials used in the aerospace industry were considered in this work. The test specimens were fabricated from the EN-AW 2024 T3 aluminium alloy and a carbon composite. It was decided to use the Naftoseal MC780 type C adhesive as a sealant to form the required hermetic, air-tight lap joints. In the definition of the joint type used, the results are presented for the tests of selected 2D and 3D surface roughness parameters, with isometric imaging of the surfaces related to this analysis. Microscopic images acquired at a magnification of x500 illustrate the surface quality. This work concludes with a discussion of the test results and conclusions.

Keywords: lap joint, aerospace structural materials, surface topography, joint sealing.

INTRODUCTION

Every machine or piece of equipment comprises a certain number of parts or components made from suitably selected materials. The parts are interconnected using a number of methods. A fixed connection is called a stationary joint, which is characterised by the parts interacting as if they were a single unit, which facilitates the production of component assemblies having a complex geometry. This in turn allows cheaper materials to be used to build large-scale assemblies, with more robust materials only being used where the greatest loads occur. The fabrication of such assemblies reduces the weight of the final product, a critical factor for the modern aerospace industry.

The second equally important type of connection is the moving joint, which can be classified into two groups: active and passive. Passive joints have one part that is stationary and does not transmit any motive power, and only permits a specific

movement by the other part. Active joints form a group of moving parts. In these joints the moment is transmitted from one part of the joint to another. Moving and stationary joints can also be classified by their fastening ability (permanent and temporary), the nature of the forces (positive and friction), and the type of connection fastener used.

Temporary joints include connections that allow parts to be connected and disconnected any number of times without the failure of either part. Permanent joints include those connections that cannot be disconnected without a failure of some parts of the joints or their fasteners.

Bonded joints have a cohesive bond, which is present between the parts being joined. Bonded joints can be made either with or without the use of a thermal energy input. In both cases, the resulting joint cannot be separated in a non-forcible way. Bonded joints can also be classified into three groups: fusion welded joints [1–3], pressure welded joints [4,5], and brazed joints [6–8].

Another group of permanent joints involves adhesive joints [9–11], where the load is transferred through the forces of adhesion [12–14]. An important consideration when analysing adhesive joints is their strength and load-bearing capacity. The strength of adhesive joints is considered by classifying them into two types: static strength and durability. Static strength is also known as short-term strength, or instantaneous strength, which ranges from a few seconds to a few dozen seconds, and sufficient testing often includes comparing the properties between the adhesive joints and to examine the factors contributing to the static strength. An extremely important advantage of adhesive joints used in the aerospace industry is the sealing of the resulting joint structure.

Hi-Lok is a simple two-piece fastener designed to achieve, in a single all-round system, design features that meet many of today's industrial requirements, in particular those applicable to the aerospace and marine sectors [15, 16]. An advantage of this fastener is the constant torque on each joined component. This is achieved through the integrated functions of a mutually interacting system. The adjustable breakoff groove in the Hi-Lok self-locking collar ensures uniform preload values by separating the torque-carrying part of the nut from the remainder of the fastener assembly, once the specified torque is achieved. The controlled preload of each Hi-Lok assembly in a structure significantly improves the fatigue life of the joined parts.

The Hi-Lok fastener must not be overloaded. This ensures that the flange is automatically shorn off when the design torque is reached. This ensures and eliminates the need to check for fastener torque. This system is highly efficient and reliable.

In many industries, structural joints are required to be airtight, as is the case in aerospace applications. The broader concept of the operating (or in-service) safety of such structures is crucial throughout the lifecycle of a machine. An important step in the design and fabrication of a lap joint using a sealant is proper substrate preparation. Important substrate preparation methods for joining modern structural materials include machining (grinding [17], burnishing [18–20], brushing [21,22]), chemical [23], electrochemical [24], ozone treatment [25] and others. As a rule, these processes are designed to develop the surface texture.

The objective of this work was to benchmark the strength of a (single) lap joint created using

a Hi-Lok fastener. The testing in this work analysed the shear strength of specimens made from the following: EN-AW 2024 T3 aluminium alloy, a carbon composite, and hybrid specimens comprising a carbon composite with EN-AW 2024 T3, joined using a Hi-Lok fastener. Tests were also carried out on specimens fabricated using the MC780 type C adhesive, which was designed to seal the structure.

EXPERIMENTAL PROCEDURE

The research plan was implemented based on a strength analysis of single-lap joint specimens made of aerospace structural materials. Test specimens fabricated from the EN-AW 2024 T3 aluminium alloy and a carbon composite were tested. The test specimen shown in Figure 1 is a single-lap specimen joined using two Hi-Lok fasteners. The dimensions of the specimens and their individual components are also shown in Figure 1.

Table 1 shows the different versions of the joints fabricated with aerospace materials (EN-AW 2024 T3 aluminium alloy and carbon composite) together with the Naftoseal MC780 Class C adhesive used as the sealant.

Strength tests were carried out on the specimens, both with and without the sealant. The EN-AW 2024 T3 aluminium alloy used in this work was a material with applications in the aerospace industry. It contained a high copper content and had good fatigue strength. It has been used in components requiring a good strength-to-weight ratio. To develop the surface of the specimens made of the EN-AW 2024 T3 aluminium alloy, a P320 grit machine tool was used. The carbon composite (six layers of carbon fiber) used in this work was fabricated in a heat and pressure (autoclave) process and is a structural material widely used in the aerospace industry. The advantage of carbon composites is their low weight, which is why there is increasing interest by the industry in this material as weight is critical in its applications. For the lap joint specimens, a Hi-Lok HL20PB-5 fastener was used, with the length specified for the stack produced (being the thickness of the single-lap specimen), and the Hi-Lok HL86PB-5 nut. Before the fabrication of the single-lap specimens, the contact faces of the structural materials were cleaned twice with acetone (by wiping and leaving to flash off).

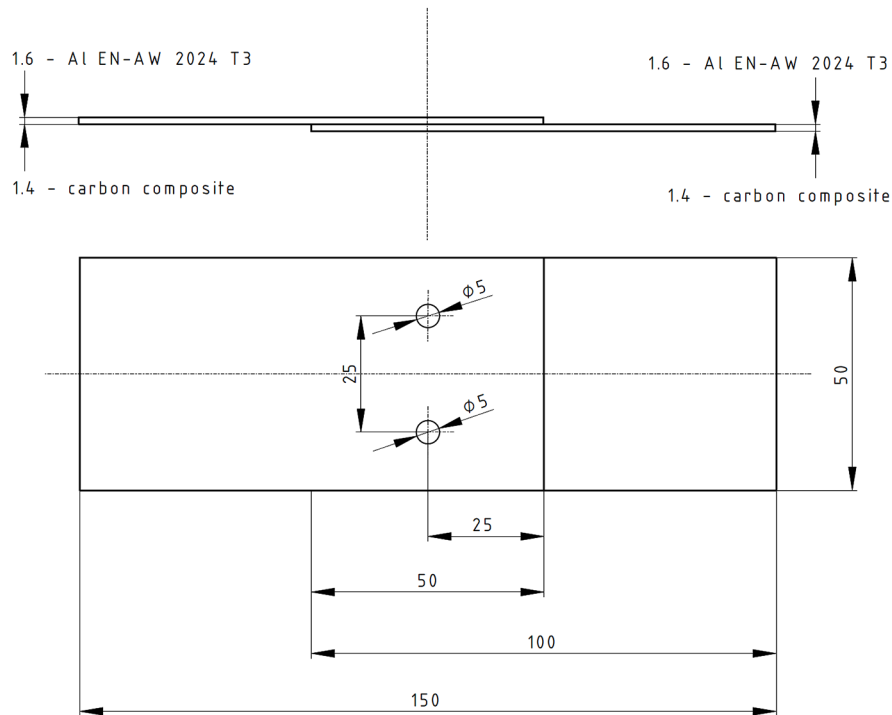


Fig. 1. Simplified schematics of the tested joint with a Hi-Lok fastener

Some of the specimens (versions V2, V4, and V6) were made with the Naftoseal MC780 Class C sealant, a two-component sealant intended for fuel tanks and air-sealing of aircraft fuselages. It was developed for the surface sealing of structures and wet riveting. It has the advantage of resistance to jet fuel and other chemicals used in the aerospace industry. It can be applied to the surfaces of materials like aluminium alloys, stainless steels, titanium alloys and composite materials without adversely affecting their strength. The test specimens (V2, V4 and V6) were fabricated as follows: the joint material was degreased in the first step of joining, followed by the hand application of the sealant. The test specimens were positioned with spring clips and left until the sealant had fully polymerised (cured). Next, the test specimens were placed in a clamp and the Hi-Lok fasteners

were installed. The samples thus fabricated were inspected for quality. The geometric dimensions of the specimens, the position of the fasteners (trueness of the holes made), the lap length, the adhesion of the shank head and nut and the sealant flash were checked, among other things. The selected surface roughness parameters (2D and 3D) were tested and analysed with a roughness and contour measurement station, a T8000 RC-120–400 from Hommel-Etamic. A 2 μm radius tip measuring probe was used for the tests.

Destructive testing was performed using a Zwick/Roell Z150 strength testing machine. The crosshead speed during the test was 2 mm/min, which means a static test range. A minimum of 5 single-lap joint specimens were produced and destroyed in each of the combinations shown (versions V1 to V6).

Table 1. Joint specimen versions

Variant	Joint assembly
V1	Carbon composite – Carbon composite
V2	Carbon composite – MC-780 Class C sealant – Carbon composite
V3	Carbon composite – Al EN-AW 2024 T3 alloy
V4	Carbon composite – MC-780 Class C sealant – Al EN-AW 2024 T3 alloy
V5	Al EN-AW 2024 T3 alloy – Al EN-AW 2024 T3 alloy
V6	Al EN-AW 2024 T3 alloy – MC-780 Class C sealant – Al EN-AW 2024 T3 alloy

A Keyence VHX-5000 microscope was also used in further examinations to ensure the quality of the specimens used and to image the surfaces of the structural materials (EN-AW 2024 T3 aluminium alloy and the carbon composite).

RESULTS AND DISCUSSION

Based on tests using selected surface roughness parameters and the analysis of the results, a suitable level of surface texture development was found for the carbon composite used. The results for the selected 2D and 3D surface roughness parameters are listed in Table 2. An adequate level of surface development is a prerequisite for the successful sealing of aerial structures. In this case, no additional treatment was required to produce a surface profile.

Table 2 includes a photograph of the carbon composite structure at a x500 magnification. The tests on selected 2D surface roughness parameters were performed for a minimum of eight test runs, and the average values of the parameters are shown on the roughness profile in the table. The results of the 3D parameter measurements are

shown in an isometric image for the surface of interest. As an analogy to the carbon composite, Table 3 shows the results of tests on selected surface roughness parameters for the EN-AW 2024 T3 aluminium alloy.

The surface of the EN-AW 2024 T3 aluminium alloy was also characterised by an adequate level of texture development. The 2D surface roughness parameters studied included: Ra – arithmetic mean of the roughness profile ordinates; Rp – maximum peak height of the roughness profile; Rv – maximum valley depth of the roughness profile; and Rz – maximum height of the roughness profile. The 3D roughness parameters studied included: Sa – arithmetic mean of the 3D profile ordinates; Sp – maximum 3D profile peak height; Sv – minimum 3D profile valley depth; and Sz – maximum 3D profile height.

Figure 2 shows the variation of forces as a function of elongation for the versions of interest (V1 to V6). The force trends shown are an example and are representative of their version group (V1 to V6). The force trends were obtained during the strength tests carried out on the Zwick/Roell Z150 machine. The crosshead speed during testing was 2 mm/min.

Table 2. Surface texture of the carbon composite

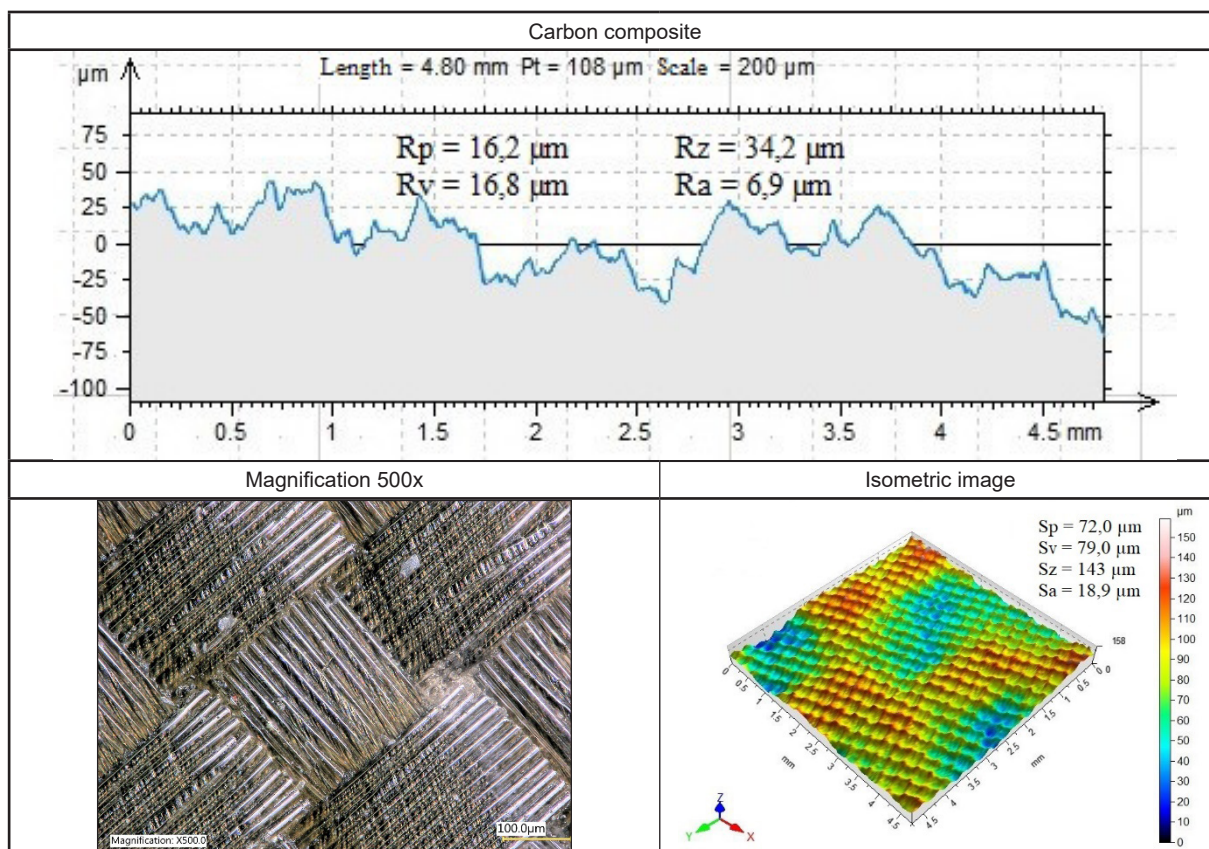
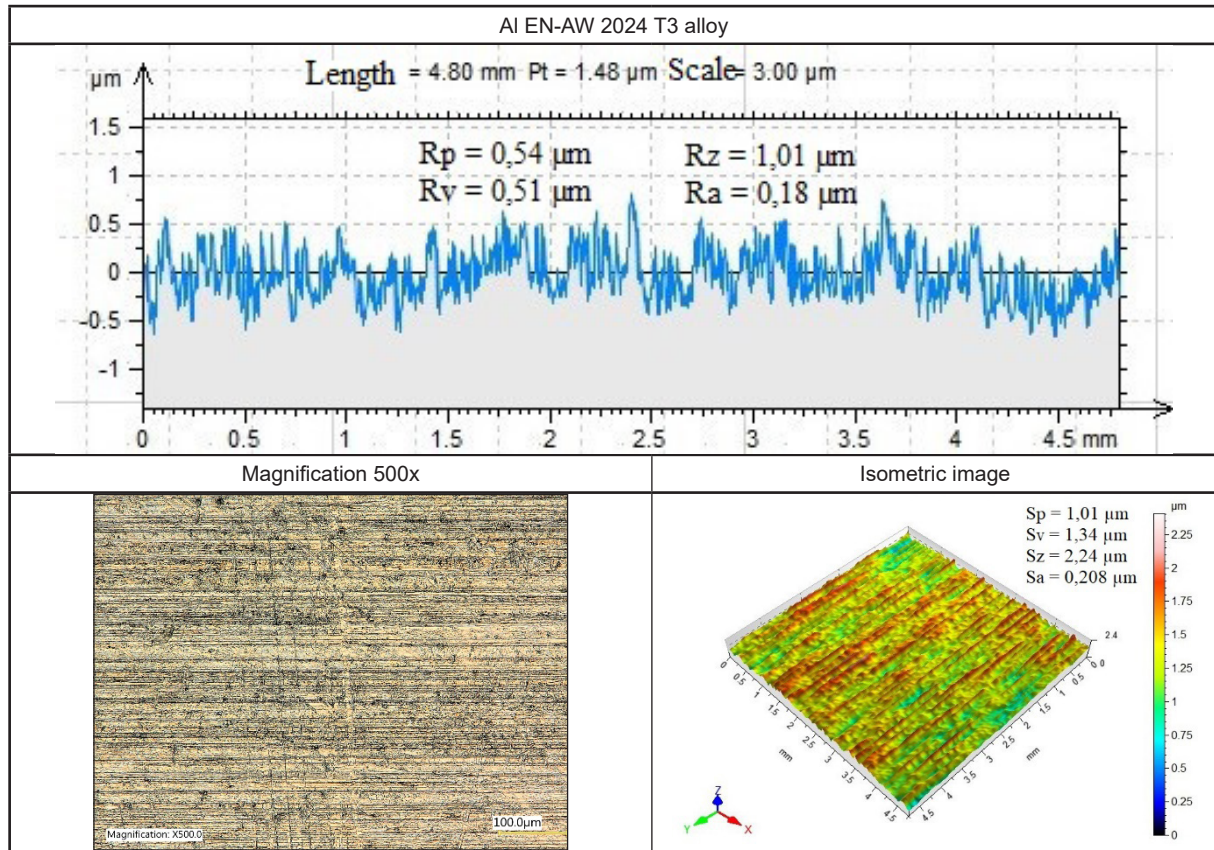


Table 3. Surface texture of the EN-AW 2024 T3 aluminium alloy



Based on the completed analysis, there is an explicit grouping found in the force variation trends. This applies to the following versions: V1-V2, V3-V4 and V5-V6. In addition to the obvious advantage of the sealant in sealing off an aerospace structure, there was an increase in the failure force of the single-lap joint (with the sealant) and an increase in the elongation of the test specimen. For the first group of versions (V1-V2), a significant increase in specimen elongation and the damping effect was observed in the specimens which featured the sealant (MC780 type C adhesive). The force trend plotted for V1 shows a characteristic failure trend of the carbon composite (the failure zone is the jagged plot line). A similar nature for the trend plots was observed for the second group of specimens (V3-V4), with a clear point of failure in carbon composite specimen V3. A slightly different nature in the force trends is represented by the third group of specimens (V5-V6), in which the single-lap joint specimen material was the EN-AW 2024 T3 aluminium alloy. Again, an increase in the failure force of the single-lap joints specimens using the MC780 type C sealant was observed, compared to the specimens without the sealant. In addition,

a point of specimen bond separation – seal loss of the structure – was found on the trend plot for version V6. Identifying this point is particularly important, especially in the aerospace industry. After a further increase in the failure force of the single-lap joint, the structure lost the seal.

Figure 3 shows the effect of the type of joint fabricated (V1 to V6) on the force level achieved during the strength tests.

Based on the results obtained, the highest failure force in the strength tests was found for the V6 test specimens, i.e. the specimens made of the EN-AW 2024 T3 aluminium alloy and sealed with the MC780 Class C adhesive.

In each group of test specimens (V1-V2, V3-V4, V5-V6), the use of the sealant in the single-lap joint resulted in a noticeable increase in the failure force of the joint, so the sealant does more than seal the structural joint. For the first group of test specimens (V1-V2) made of the carbon composite, a 12% increase in failure force was found for the specimens with the sealant compared to the specimens without the sealant. For the hybrid specimens (V3-V4), a 15% increase in failure strength was found for the specimens with the sealant compared

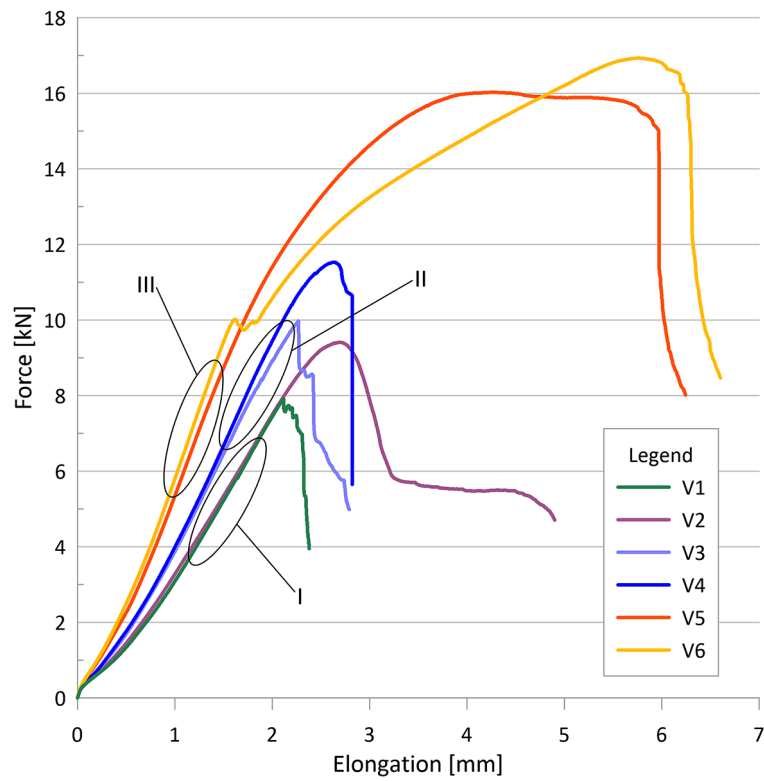


Fig. 2. Force variation trend vs. elongation for the versions tested

to those without the sealant. As a measure of the scatter in the results, the standard deviation values are shown in Figure 3. It is worth noting these values, as they were relatively low for

all the specimen types tested, which is indicative of the repeatability of the single-lap joints. Table 4 summarises the examples of failures in the structural single-lap joints.

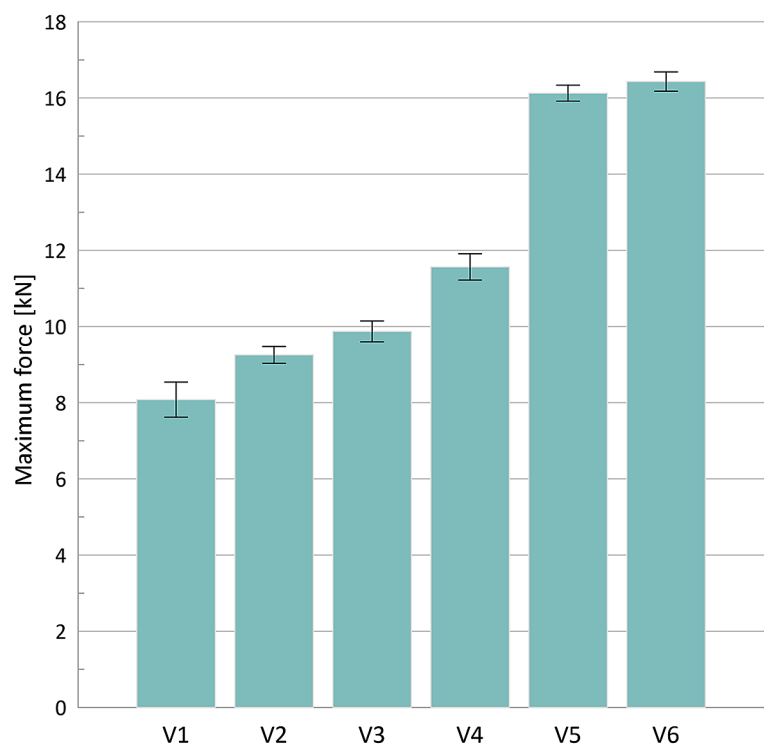
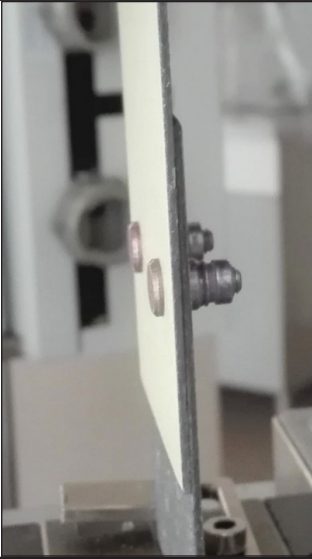


Fig. 3. Fabricated joint type (V1 to V6) vs. structural failure force

Table 4. Failure examples of a structural material single-lap joint

Variant V1	Variant V2
	
Variant V3	Variant V4
	
Variant V5	Variant V6
	

The images in Table 4 show all the sample combinations analysed during this work. The failure zones of the specimens are evident in these images.

CONCLUSIONS

Based on all the work carried out, certain general conclusions can be made. The surface of the carbon composite does not require preparation for the adhesive bonding processes. The level of surface texture development was sufficient. In all test specimens made with the MC780 Type C adhesive as a sealant, an increase in the failure force of the single-lap joint was found, in comparison to the specimens without this sealant. The largest increase of 15% was found in hybrid versions V3-V4 of the specimens tested. Based on the tests, relatively small scatter values of the test results around the mean value were determined, which indicates a stable fabrication process for single-lap joints. The analysis facilitated a statement about the grouping of the force variation trends. This applies to these versions: V1-V2, V3-V4 and V5-V6.

REFERENCES

1. Tomków J, Landowski M, Rogalski G. Application Possibilities Of The S960 Steel In Underwater Welded Structures. *Fu Mech Eng* 2022; 20: 199. <https://doi.org/10.22190/FUME210722066T>
2. Ghiasvand A, Noori SM, Suksatan W, Tomków J, Memon S, Derazkola HA. Effect of Tool Positioning Factors on the Strength of Dissimilar Friction Stir Welded Joints of AA7075-T6 and AA6061-T6. *Materials* 2022; 15: 2463. <https://doi.org/10.3390/ma15072463>.
3. Janeczek A, Tomków J, Fydrych D. The Influence of Tool Shape and Process Parameters on the Mechanical Properties of AW-3004 Aluminium Alloy Friction Stir Welded Joints. *Materials* 2021; 14: 3244. <https://doi.org/10.3390/ma14123244>.
4. Kubit A, Trzepieciński T, Święch Ł, Faes K, Słota J. Experimental and Numerical Investigations of Thin-Walled Stringer-Stiffened Panels Welded with RFSSW Technology under Uniaxial Compression. *Materials* 2019; 12: 1785. <https://doi.org/10.3390/ma12111785>.
5. Kubit A, Trzepieciński T, Kluz R, Ochalek K, Słota J. Multi-Criteria Optimisation of Friction Stir Welding Parameters for EN AW-2024-T3 Aluminium Alloy Joints. *Materials* 2022; 15: 5428. <https://doi.org/10.3390/ma15155428>.
6. Wang P, Lin J, Xu Z, Qin B, Cao J, Feng J, et al. Negative thermal expansion of Sc₂W₃O₁₂ interlayer with three-dimensional interpenetrating network structure for brazing C/SiC composites and GH3536. *Carbon* 2023; 201: 765–75. <https://doi.org/10.1016/j.carbon.2022.09.072>.
7. Xv W, Wang S, Cai L, Zhang X, Dou Z, Luo W. Brazing and magnetic properties control of sintered NdFeB permanent magnet with high coercivity. *Scripta Materialia* 2022; 221: 114971. <https://doi.org/10.1016/j.scriptamat.2022.114971>.
8. Niyaraki MN, Nouri MD. Investigation of microstructure and mechanical behavior of AISI420/BNi-2 brazed joints under impact loading at high strain rates with the split Hopkinson bar. *Weld World* 2022; 66: 1957–73. <https://doi.org/10.1007/s40194-022-01325-1>.
9. Kłonica M, Kuczmazewski J, Samborski S. Effect of a Notch on Impact Resistance of the Epidian 57/Z1 Epoxy Material after “Thermal Shock.” *SSP* 2015; 240: 161–7. <https://doi.org/10.4028/www.scientific.net/SSP.240.161>.
10. Houjou K, Akiyama H, Sato C. Fatigue fracture behavior of cured epoxy adhesive containing a surface crack. *Polymer Testing* 2023; 117: 107821. <https://doi.org/10.1016/j.polymertesting.2022.107821>.
11. Rocha J, Sena-Cruz J, Pereira E. Influence of adhesive stiffness on the post-cracking behaviour of CFRP-reinforced structural glass beams. *Composites Part B: Engineering* 2022; 247: 110293. <https://doi.org/10.1016/j.compositesb.2022.110293>.
12. Kłonica M. Analysis of the effect of selected factors on the strength of adhesive joints. *IOP Conf Ser: Mater Sci Eng* 2018; 393: 012041. <https://doi.org/10.1088/1757-899X/393/1/012041>.
13. Kłonica M. Comparative Analysis Of Effect Of Thermal Shock On Adhesive Joint Strength. *Adv Sci Technol Res J* 2016; 10: 263–8. <https://doi.org/10.12913/22998624/66509>.
14. Skoczylas J, Samborski S, Kłonica M. A multilateral study on the FRP Composite’s matrix strength and damage growth resistance. *Composite Structures* 2021; 263: 113752. <https://doi.org/10.1016/j.compstruct.2021.113752>.
15. iang J, Xi F (Jeff), Bi Y. Design and Analysis of a Robotic End-Effector for Automated Hi-Lok Nut Installation. *Coatings* 2022; 12: 904. <https://doi.org/10.3390/coatings12070904>.
16. Hardy DF, DuQuesnay DL. Effect of Repetitive Collar Replacement on the Residual Strength and Fatigue Life of Retained Hi-Lok Fastener Pins. *Metals* 2019; 9: 445. <https://doi.org/10.3390/met9040445>.

17. Frutos E, Richhariya V, Silva FS, Trindade B. Manufacture and mechanical-tribological assessment of diamond-reinforced Cu-based coatings for cutting/grinding tools. *Tribology International* 2023; 177: 107947. <https://doi.org/10.1016/j.triboint.2022.107947>.
18. Matuszak J, Zaleski K, Skoczylas A, Ciecieląg K, Kęcik K. Influence of Semi-Random and Regular Shot Peening on Selected Surface Layer Properties of Aluminum Alloy. *Materials* 2021; 14: 7620. <https://doi.org/10.3390/ma14247620>.
19. Zaleski K, Skoczylas A, Brzozowska M. The Effect Of The Conditions Of Shot Peening The Inconel 718 Nickel Alloy On The Geometrical Structure Of The Surface. *Advances in Science and Technology Research Journal* 2017; 11: 205–11. <https://doi.org/10.12913/22998624/74180>.
20. Świetlicki A, Szala M, Walczak M. Effects of Shot Peening and Cavitation Peening on Properties of Surface Layer of Metallic Materials – A Short Review. *Materials* 2022; 15: 2476. <https://doi.org/10.3390/ma15072476>.
21. Matuszak J. Effect of Ceramic Brush Treatment on the Surface Quality and Edge Condition of Aluminium Alloy after Abrasive Waterjet Machining. *Advances in Science and Technology Research Journal* 2021; 15: 254–63. <https://doi.org/10.12913/22998624/140336>.
22. Matuszak J, Zaleski K. Analysis of deburring effectiveness and surface layer properties around edges of workpieces made of 7075 aluminium alloy. *Aircraft Engineering and Aerospace Technology* 2018; 90: 515–23. <https://doi.org/10.1108/AEAT-05-2016-0074>.
23. Szala M, Hejwowski T. Cavitation Erosion Resistance and Wear Mechanism Model of Flame-Sprayed Al₂O₃–40%TiO₂/NiMoAl Cermets Coatings. *Coatings* 2018; 8: 254. <https://doi.org/10.3390/coatings8070254>.
24. Vijayakumar P, Valarselvan S, Abuthahir SSS. Corrosion Resistance, Electrochemical and Surface Morphology Studies of Mild Steel in a Sulphuric Acid Medium by using Dibutyl Sulphide: *Port Electrochim Acta* 2023; 41: 1–15. <https://doi.org/10.4152/pea.2023410101>.
25. Kłonica M. Application of the Ozonation Process for Shaping the Energy Properties of the Surface Layer of Polymer Construction Materials. *Journal of Ecological Engineering* 2022. <https://doi.org/10.12911/22998993/145265>.